SAND2022-8695C

The isothermal oxidation of high-purity aluminum foil at high temperature: temperature-dependent rates and energetics

Eric N. Coker, Burl Donaldson, and Walter Gill
Sandia National Laboratories
P.O. Box 5800
Albuquerque, New Mexico 87185
USA

Abstract

The isothermal oxidation in air of high-purity Al foil was studied as a function of temperature using Thermogravimetric Analysis simultaneously with Differential Scanning Calorimetry (TGA/DSC). The rates and extents of oxidation were found to be non-linear functions of the temperature, in agreement with the literature. Between 650 and 750 °C very little oxidation took place; at 850 °C oxidation occurred after an induction period, while at 950 °C oxidation occurred without an induction period. At oxidation temperatures between 1050 and 1150 °C rapid passivation of the surface of the aluminum foil occurred, while at 1250 °C and above, an initial rapid mass increase was observed, followed by a more gradual increase in mass. The initial rapid increase in mass was accompanied by a significant exotherm, which was quantified by DSC. At temperatures of 1050 °C and above the specimen coalesced into a spheroidal particle, whereas at lower temperatures the original foil morphology was retained due to the cohesive strength of the native oxide layer. Cross-sections of oxidized specimens were characterized by scanning electron microscopy (SEM); the observed alumina skin thicknesses correlated qualitatively with the observed mass increases. Interrogation of the surface of an oxidized spheroidal particle by SEM showed a fractured alumina shell around a partially hollow core of Al which appeared to have grain boundaries.

INTRODUCTION

A considerable body of work exists describing the oxidation or ignition of aluminum particles at elevated temperature. The particulate sources, while being representative of commercial products, suffer from broad particle size ranges (hence varying surface areas) and varying levels of impurities. To gain a clearer scientific understanding of the processes involved in the air-oxidation of Al, high purity, low specific surface area foil was used in the present study. An additional level of control used in the current work (but absent in most previously published work) was to initiate oxidation once the specimen had stabilized at the desired oxidation temperature, i.e., the initial heat-up and stabilization was carried out under high purity inert gas stream.

In general, the oxidation of aluminum in air can be described as occurring in four distinct stages. Reference [1] includes a diagram (their Figure 1) which illustrates these oxidation stages clearly, and in-situ X-ray diffraction has been used to monitor the phase changes occurring in the Al/Al_2O_3 system during heat treatment in air.[2]

The native amorphous alumina layer covering a particle of Al (present even at room temperature) initially grows extremely slowly during the low temperature oxidation stage I, which extends up to about 550 °C. The rate of this process is believed to be controlled by the outward diffusion of Al cations.[3] The amorphous oxide remains stable, due to the energy of the oxide–metal interface, only up to a critical thickness of about 5 nm.[4,5] The amorphous oxide transforms into γ-alumina once the critical thickness is approached or when the temperature becomes sufficiently high. Since the density of γ-alumina is greater than that of amorphous alumina,[6] and the smallest γ-alumina crystallites have a size of about 5 nm,[7] if the thickness of the amorphous layer was less than 5 nm, the newly formed γ-alumina crystallites are no longer able to form a continuous layer covering the aluminum surface. Consequently, the beginning of stage II (ca. 550 °C) is accompanied by an increase in the rate of oxidation, and as the openings in the oxide coating heal the rate of oxidation decreases. By the end of stage II at around 650 °C, a polycrystalline layer of γ-alumina has formed that covers the entire surface of the aluminum. During stage III (approximately 650 – 1050 °C) the growth of γ-alumina continues at a rate which is limited by the inward diffusion of oxygen anions along grain boundaries.[3,8] Growth of the γ-alumina layer can be accompanied by phase transformations into other transition polymorphs, such as δ-alumina and θ-alumina. Due to the similarity in density of these polymorphs with γ-alumina,[6] such transitions are not expected to affect the oxidation rate significantly. At sufficiently high temperature the transition alumina polymorphs become destabilized, and begin to convert to α-alumina, indicating the end of Stage III. When the first α-alumina crystallites begin to form at the end of stage III, the thickness of the γ-alumina layer decreases due to the greater density of the α-alumina phase (a volume contraction of 13.8% is expected[9] on converting γ-alumina to α-alumina), and the oxidation rate increases momentarily. Stage IV is considered to start when the oxide scale is completely transformed to α-alumina, at about 1050 °C. Once most of the oxide layer is transformed to coarse and dense α-alumina crystallites resulting in continuous polycrystalline coverage, grain boundary diffusion slows down, and the oxidation rate decreases rapidly.

EXPERIMENTAL DETAILS

The aluminum foil was obtained from Johnson Matthey, and had a purity of 99.998% and a thickness of 0.5mm. A steel punch was used to cut out circular specimens with a diameter of ~ 4.9 mm from the Al foil sheet. The circular specimens fit snugly into the bottom of high-purity alumina crucibles, and had a mass of about 26 mg. The specimens were characterized under inert atmosphere (UHP argon) and oxidizing atmosphere (75% ultra-zero air – 25% UHP argon) with TGA/DSC (Netzsch STA 449-F3 Jupiter) during heating under argon to a pre-determined temperature and oxidizing at that temperature for a set amount of time. Total gas flow rates were maintained at 160 sccm throughout each experiment. In all experiments, a heating rate of 20 °C min^{-1} was used from ambient to 600 °C, and from 700 °C to the final oxidation temperature. In the range 600 to 700 °C a rate of 5 °C min^{-1} was used to enable accurate monitoring of the Al melting temperature (660.3 °C; used as an internal temperature standard). For the experiment in which oxidation occurred at 650 °C, the sample was first heated to 700 °C then cooled down to 650 °C. In all experiments, the specimen was heated under inert atmosphere to the desired oxidation temperature, and was allowed to stabilize at that temperature under flowing inert gas for 15 min prior to initiating air flow.

All TGA/DSC data have been corrected by baseline subtraction. In order to do this, blank experiments (empty crucibles) were run under exactly the same conditions as the experimental runs, and the blank data was then subtracted from the experimental data. Prior to starting each TGA/DSC experiment, the instrument was evacuated and back-filled with argon three times, then allowed to sit idle under the gas flow conditions to be used in the experiment for at least 15 minutes to ensure a clean, consistent atmosphere and stable balance reading and DSC signal at the start of each run.

Scanning Electron Microscope (SEM) images were acquired using a JEOL JXA-5900LV, with a Noran System 7 EDS. Specimens were either potted in epoxy resin, then cut and polished to reveal a cross-section of the particle, or imaged without potting to observe surface features.

RESULTS AND DISCUSSION

Thermogravimetric Analysis – Differential Scanning Calorimetry

The TGA data in Figure 1 shows the oxidation behavior versus time during isothermal holds at temperatures between 650 and 1550 °C. Time zero is defined as the point at which air was first introduced into the TGA, and the data plotted begins 10 minutes before t = 0. The observed behavior (i.e., oxidation mass change versus temperature of exposure to air) is directly comparable to previous literature reports where Al samples were heated at various rates under oxidizing conditions, described in the introduction. One significant difference between the present and most of the earlier work is that in the present work the temperature range for stage I (growth of amorphous oxide layer) was traversed without exposure of the sample to an oxidizing environment; air was introduced in one of the later stages, using the definitions given in the introduction.

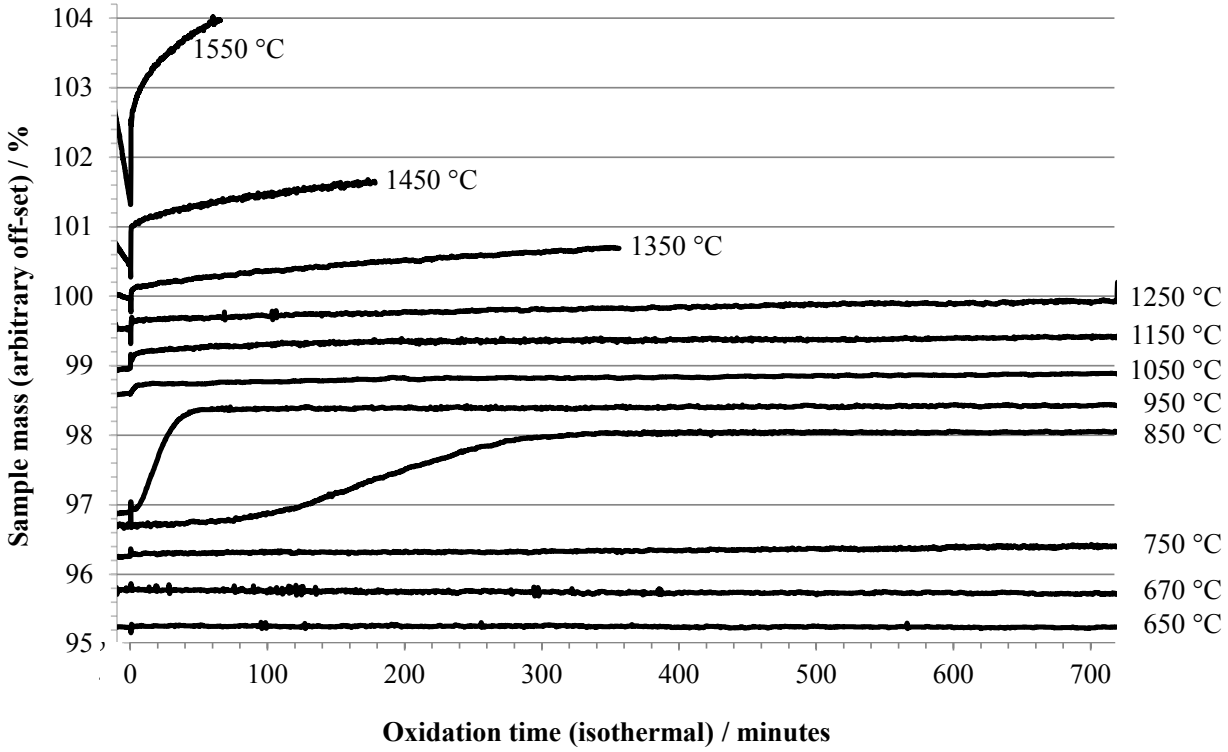

Figure 1. TGA results for Al foil heated under argon to the indicated temperature, then exposed to air (at t = 0).

The TGA data recorded during oxidation at 650 and 670 °C showed negligible mass increase during a 12 hr hold (Figure 1). At an oxidation isotherm of 750 °C, the onset of slow oxidation was observed, while at 850 °C a gradual mass increase occurred with a rate that initially accelerated and became significant after about 1 hr of exposure to air. A similar induction period was reported by Bergsmark, et al., for commercial-grade Al (>1500 ppm impurity level) at 850 °C under pure oxygen.[10] Kolarik, et al.[2] observed the delayed transformation of γ-alumina to α-alumina by in

situ XRD after holding for 160 minutes in air at 850 °C. At 950 °C a similar overall mass increase was seen, but at a more rapid rate and without a significant induction period. The observations of TGA data in this temperature range are consistent with stage III oxidation. The induction period seen at 850 °C may be a consequence of the necessity to build up a contiguous layer of γ-alumina on the specimen prior to transition to δ-, θ-, and eventually α-polymorphs, and that the buildup of γ-alumina is slow at 850 °C.

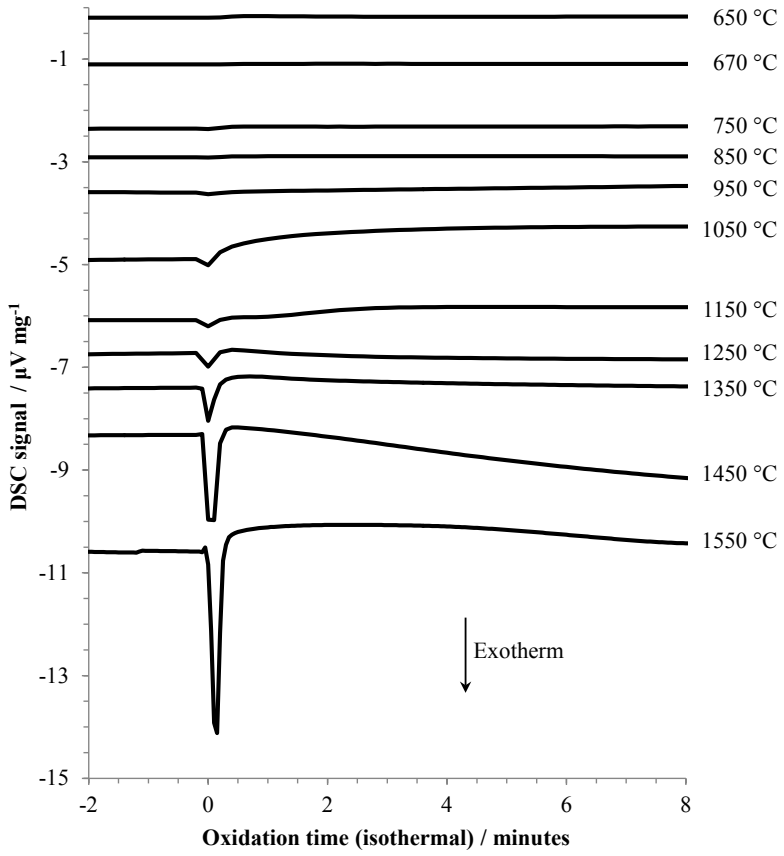

Figure 2. DSC results for Al foil heated under argon to the indicated temperature, then exposed to air (at t = 0).

The slow, but gradually increasing (with temperature) oxidation at 1050, 1150, and 1250 °C coincides with the transition from stage III into stage IV oxidation. At 1350 °C and above, the rate of oxidation becomes increasingly significant. Two other factors are apparent at the highest oxidation temperatures, 1) the sample mass decreases during the isothermal hold before air is admitted, and 2) there is a large, almost instantaneous increase in mass upon initial exposure to air, followed by a more gradual increase. This rapid increase in mass is accompanied by a significant exotherm, as shown in Figure 2. At oxidation temperatures below 1050 °C the exotherm was barely noticeable. Figure 3 plots the energy released during the initial rapid oxidation event, based upon the measured peak intensity (area) for each exotherm, against oxidation temperature.

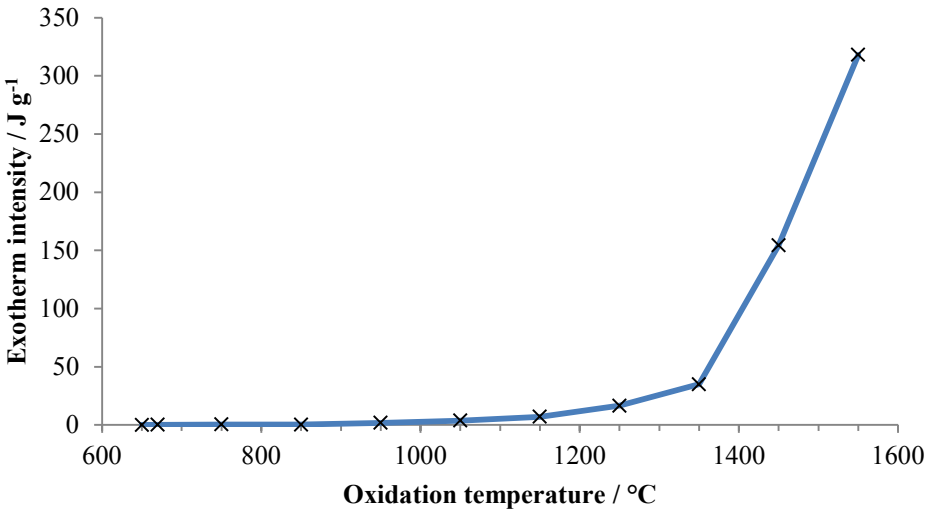

Figure 3. Energy released upon first exposure of Al foil to air versus temperature of exposure. Energy is normalized to the total specimen mass at the beginning of the experiment.

The decreasing mass prior to oxidation at the highest temperatures is ascribed to vaporization of aluminum. Figure 4 shows an expansion of the region around the introduction of air for experiments conducted at oxidation temperatures of 1350, 1450, and 1550 °C. It can be seen that vaporization becomes noticeable slightly below 1350 °C, and the rate increases rapidly with temperature.

The rates of mass loss seen in Figure 4 were calculated for the linear portions of the mass change curves during evaporation of Al, and these are plotted in Figure 5 together with data for the vapor pressure of Al at similar temperatures. Not surprisingly, there is good correlation between the trend of rate of mass loss due to evaporation of Al and the reported vapor pressures. The mass loss rate and vapor pressure increase approximately exponentially with temperature.

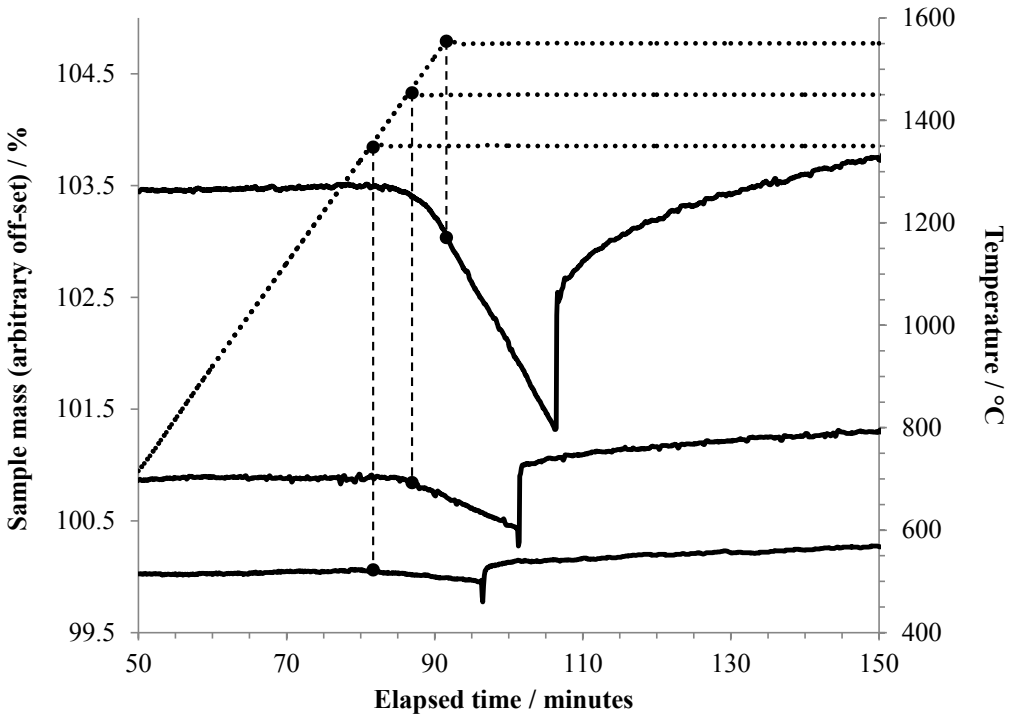

Figure 4. TGA results for Al foil heated to 1350 °C or higher under argon, held at that temperature for 15 minutes, then exposed to air. The vertical dashed lines tie the respective TGA curves to the point on the temperature curve (dotted line) where the isothermal hold began. In this plot, the beginning of each experiment is taken as t = 0. The point at which air flow began is recognized by the sudden mass increase in each curve.

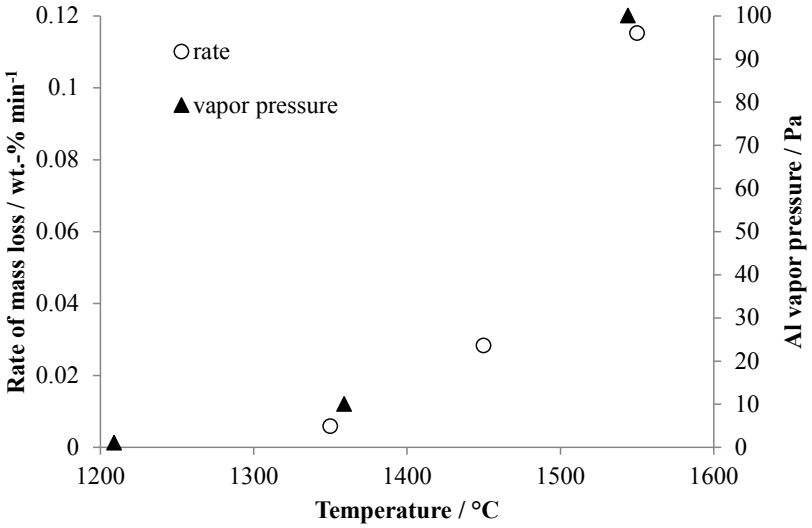

Figure 5. Rates of mass loss during Al evaporation taken from Figure 4 compared to the published vapor pressure of Al at similar temperatures. The Al vapor pressure data was taken from http://www.knowledgedoor.com/2/elements_handbook/vapor_pressure.html.

Scanning Electron Microscopy

Samples of Al foil which had been oxidized at temperatures between 750 and 1550 °C were potted in epoxy resin and sectioned with a diamond saw to reveal cross-sections of the specimens. These were then imaged in a scanning electron microscope. Representative images depicting the alumina shell that formed upon oxidation for the various specimens are shown in Figure 6. The non-linear variation with oxidation temperature of alumina shell thickness is apparent, as is the change in shell morphology with temperature. Based upon the images, an estimate was made of the thickness of the alumina shell for each specimen, and the results are plotted in Figure 7. Also in Figure 7 are the total mass increases upon oxidation recorded by TGA for the various specimens. The qualitative agreement between the two sets of data is quite good, despite the large uncertainties associated with estimating the thickness of such irregular shell structures.

Despite the fact that all of the specimens shown in Figure 6 were oxidized at a temperature above the melting point of Al, only those heated to 1050 °C or higher formed into spheroidal droplets. The specimens oxidized at 950 °C or below each retained the overall morphology of the initial foil, presumably due to the stabilizing nature of the native oxide layer which resists fragmentation at the lower temperatures. At the higher temperatures reorganization of the alumina shell does occur; this may be a function of increasing flexibility of the alumina with temperature, expansion of the molten aluminum core, increased vapor pressure of aluminum causing fragmentation of the shell, and/or recrystallization of the alumina at higher temperatures allowing facile restructuring of the shell architecture.

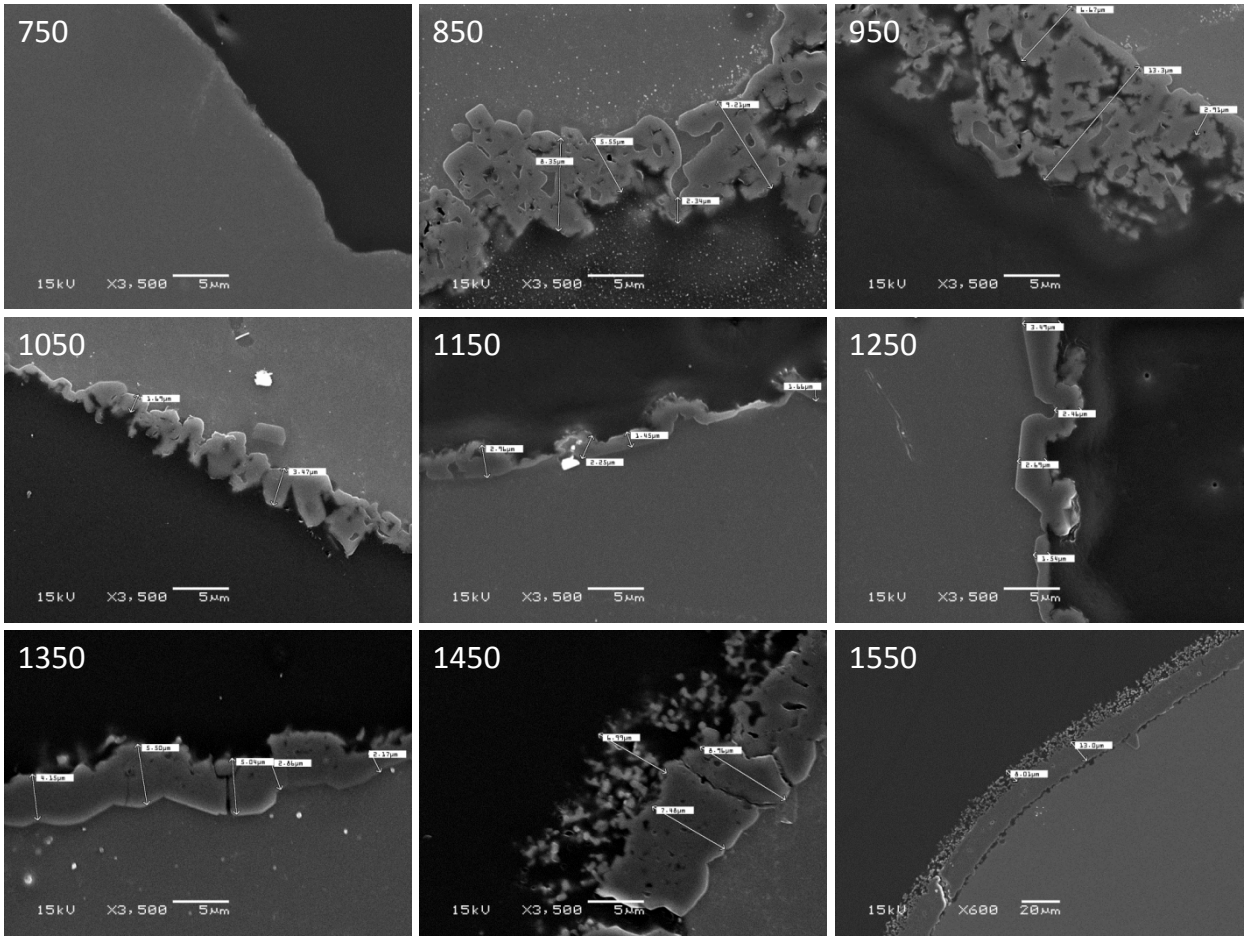

Figure 6. SEM images of cross sections of Al foil specimens after oxidation in air at the indicated temperature (in °C). Note that all images are shown at the same magnification (scale bar = 5 µm), except for that of the specimen oxidized at 1550 °C (scale bar = 20 µm).

The outer surface of the alumina shell of a non-sectioned Al/alumina sphere produced by oxidizing Al foil at 1050 °C for 12 hours was imaged in the SEM, and representative images are shown in Figure 8. Figures 8A and C show the spheroidal nature of the specimen and areas where the alumina shell collapsed (presumably upon cooling, due to differences in thermal expansion coefficients for Al versus alumina). Chemical analysis in the SEM using energy dispersive spectroscopy indicated that the outer surface was alumina (rich in both Al and oxygen), while the exposed interior of the sphere was rich in Al but contained less oxygen. Figure 8B shows what looks like grain boundaries in the internal Al-rich zone, suggesting that crystallization of the molten Al into discrete crystallites occurred upon cooling. Figure 8D shows a close-up of the surface texture, and it appears that dendritic-type growth of alumina occurred on top of a smoother initial coating of alumina on the Al particle.

The formation of partially hollow alumina spheres during oxidation of micron-sized Al particles has been documented,[2] and forms the basis for certain enhanced anti-corrosion coating technologies.

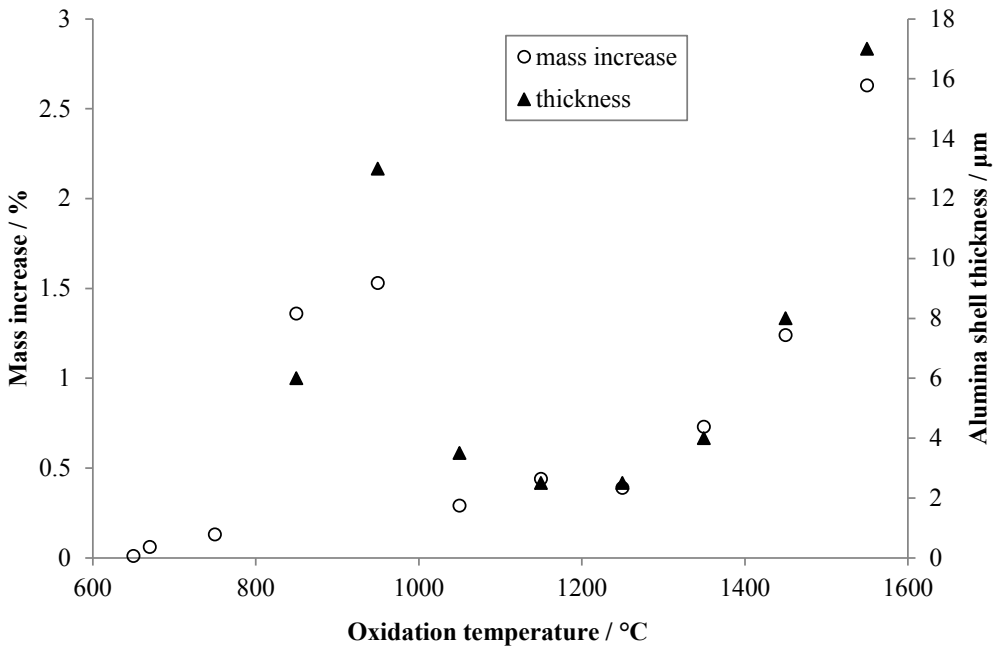

Figure 7. Thicknesses of the alumina shells estimated from the images shown in Figure 6 (filled triangles), and total mass gain during oxidation for each specimen recorded by TGA (open circles). Arbitrary scaling has been applied to both y-axes to visually align the two data sets.

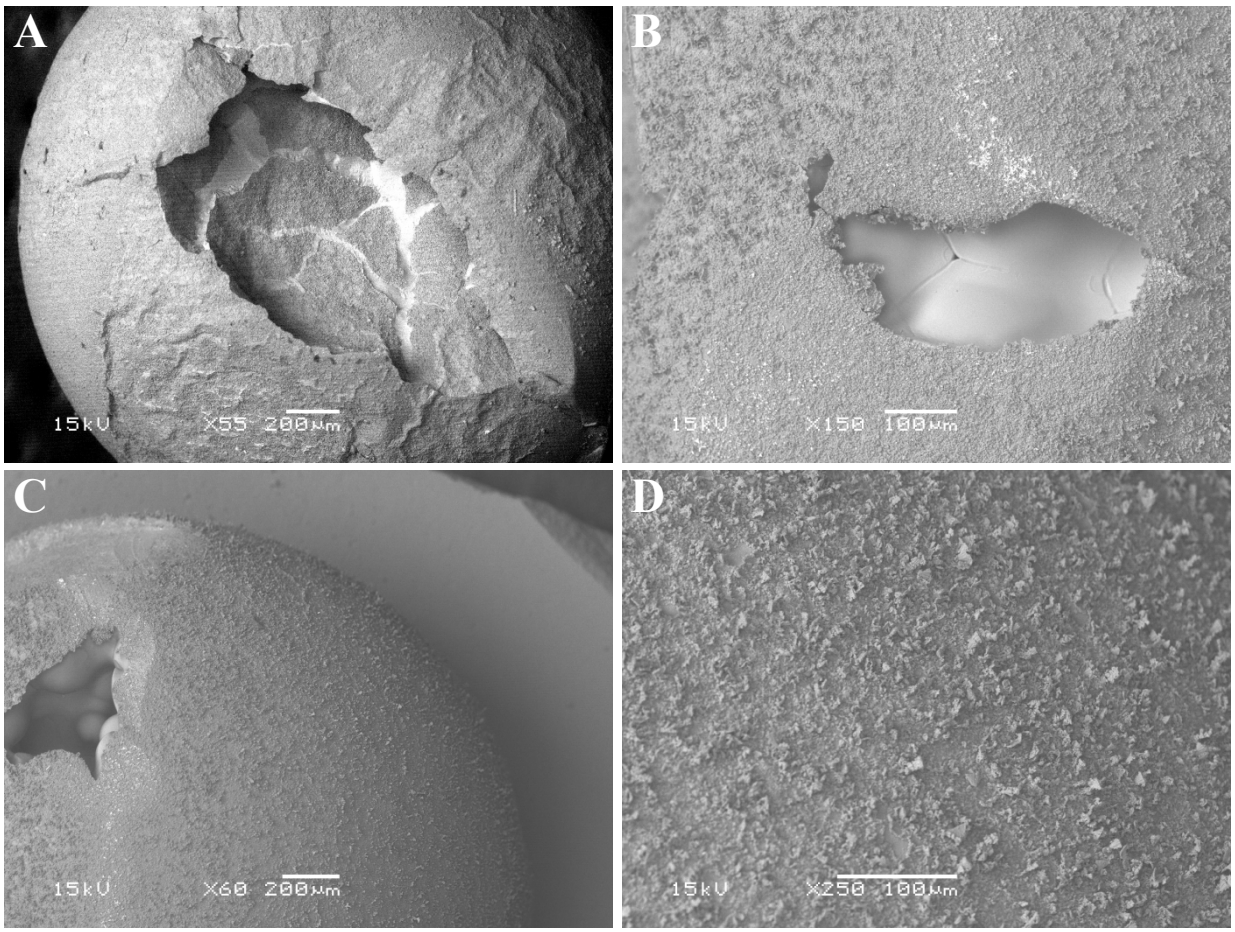

Figure 8. SEM images the outer surface of an Al foil specimen after oxidation in air at 1050 °C for 12 hours.

CONCLUSIONS

In the isothermal oxidation experiments described in this paper the rate or extent of oxidation in air was found to be not a linear function of the temperature, rather different temperature ranges resulted in different behavior, in agreement with the literature. Specifically, at the lowest temperatures studied (between 650 and 750 °C) very little oxidation took place, even after 12 hr exposure to air. At 850 °C oxidation occurred after an induction period, while at 950 °C a similar amount of oxidation occurred as at 850 °C, but without a significant induction period. Raising the temperature further resulted in rapid passivation of the surface of the aluminum foil, as only small and gradual mass increases were measured at oxidation temperatures of 1050, 1150, and 1250 °C. Although the amounts of oxidation occurring at these three temperatures were very small, it was observed that the rates of mass increase changed proportionally with temperature. At 1250 °C and above, an initial extremely rapid mass increase was observed (the magnitude of which increased with increasing temperature), followed by a more gradual increase in mass. The initial rapid increase was accompanied by a significant exotherm as measured by DSC. At temperatures of 1350 °C and above, mass loss was recorded during the ramp up to oxidation temperature under inert atmosphere; the mass loss began at about 1350 °C, and became significant above 1400 °C. This is attributed to vaporization of aluminum. Oxidized Al foil samples were mounted in epoxy

resin and cross-sectioned for characterization by scanning electron microscopy (SEM); the observed alumina skin thicknesses correlated qualitatively with the observed mass increases for each oxidation temperature studied. Interrogation by SEM of the outer surface of a spheroidal particle produced by oxidation of an Al foil specimen at 1050 °C revealed a partially-hollow sphere of Al, with a fractured outer alumina shell. Specimens oxidized at temperatures below 1050 °C did not transform into spheroidal particles, rather they retained the overall morphology of the foil, presumably due to the stabilizing effect of the native alumina shell at these temperatures.

ACKNOWLEDGMENTS

The work described herein was sponsored by the Sandia National Laboratories Weapons Systems Engineering Assessment Technology (WSEAT) Program. The SEM work was carried out by Richard Grant and Amy Allen, and specimens were prepared for SEM by Alice Kilgo. Sandia National Laboratories is a multi-mission laboratory managed and operated by National Technology and Engineering Solutions of Sandia, LLC., a wholly owned subsidiary of Honeywell International, Inc., for the U.S. Department of Energy's National Nuclear Security Administration under contract DE-NA0003525.

REFERENCES

1 Trunov, M.A., Schoenitz, M. and Dreizin, E.L., **2006**, Effect of polymorphic phase transformations in alumina layer on ignition of aluminium particles. *Combustion Theory and Modelling*, **10(4)**, 603-23

2 Kolarik, V., del Mar Juez-Lorenzo, M. and Fietzek, H., **2011**, Oxidation of micro-sized spherical aluminium particles. *Mater. Sci. Forum*, **696**, 290-5.

3 Jeurgens, L.P.H., Sloof, W.G., Tichelaar, F.D. and Mittemeijer, E.J., **2002**, Growth kinetics and mechanisms of aluminum oxide films formed by thermal oxidation of aluminum. *J. Appl. Phys*., **92**, 1649–56.

4 Jeurgens, L.P.H., Sloof, W.G., Tichelaar, F.D. and Mittemeijer, E.J., **2000**, Thermodynamic stability of amorphous oxide films on metals: application to aluminum oxide films on aluminum substrates. *Phys. Rev. B*, **62**, 4707–19.

5 Jeurgens, L.P.H., Sloof, W.G., Tichelaar, F.D. and Mittemeijer, E.J., **2002**, Structure and morphology of aluminum-oxide films formed by thermal oxidation of aluminum. *Thin Solid Films*, **418**, 89–101.

6 Levin, I. and Brandon, D., **1998**, Metastable alumina polymorphs: Crystal structures and transitions sequences. *J. Am. Ceram. Soc*., **81**, 1995–2012.

7 Dwivedi, R.K. and Gowda, G., **1985**, Thermal stability of aluminum oxides prepared from gel. *J. Mater. Sci. Lett*., **4**, 331–43.

8 Riano, O.A., Wadsworth, J. and Sherby, O.D., **2003**, Deformation of fine-grained alumina by grain boundary sliding accommodated by slip. *Acta Materialia*, **51**, 3617–34.

9 Sibota, N.N. and Shokhina, G.N., **1974**, *Kristall und Technik*, **9**, 913-9.

10 Bergsmark, E., Simensen, C.J. and Kofstad, P., **1989**, The oxidation of molten aluminium. *Mater. Sci. Eng*., **A120**, 91-5.